Forensic Science International: Reports 7 (2023) 100321

Contents lists available at ScienceDirect

Forensic Science International: Reports

journal homepage: www.sciencedirect.com/journal/forensic-science-international-reports

Predicted changes to the rate of human decomposition due to climate change during the 21st century

Julius Strack [a,b], Martin J. Smith [a,*]

[a] Department of Anthropology and Archaeology, Bournemouth University, Fern Barrow, Poole BH12 5BB, United Kingdom
[b] Institute for Legal Medicine, University Medical Center Hamburg-Eppendorf, Butenfeld 34, 22527 Hamburg, Germany

ARTICLE INFO

Keywords:
Post mortem Interval
Climate change
Decomposition
Forensic Anthropology
Modelling

ABSTRACT

Estimating the post mortem interval is an important aspect of the work of forensic pathologists and forensic anthropologists. Whilst temperature is generally agreed as the most important variable affecting decomposition, some formulae also incorporate relative humidity for a more detailed estimate. Both these variables are impacted by anthropogenic climate change. This study aims to provide a first overview of the likely extent to which anthropogenic climate change will affect future rates of decomposition. The post mortem interval from death until skeletonization (PMIDS) was calculated using the formula by Vass [1], as well as temperature and humidity predictions from two different climate models, to predict changes in the speed of decomposition between the decades 2020–2029 and 2090–2099. The changes are calculated for different climate zones, and a global average, as well as different climate change scenarios, and for decomposition starting in January and July. The estimated PMIDS is significantly ($p < 0.05$) decreased in most scenarios, with the largest global decrease of 33.5% in the SSP5–8.5 scenario, with decomposition starting in July, and the smallest decrease of 2.6% in the SSP1–2.6 scenario, with decomposition starting in January. The significantly accelerated decomposition in the SSP5- 8.5 scenario will increase the workload of forensic anthropologists, by decreasing the time until skeletonization, after which the expertise of a forensic anthropologist is more likely to be needed. However, climate change is also predicted to decrease the accuracy of the formulae used for PMI estimation, even in regions where levels of precision are currently good. The present authors therefore argue, that the impacts of climate change will warrant increasing attention in the field of forensic anthropology, and that more research into PMI estimation will be needed particularly in warmer and drier regions.

Introduction

Estimation of the post mortem interval (PMI) plays an important role in Forensic Death Investigations. The PMI can help with the identification process, and is important for building a timeline, and testing alibis for potential suspects [2]. In forensic anthropology, the two most commonly used (self-acclaimed) 'universal' formulae for PMI estimation are the formulae by Megyesi et al. and Vass. Both formulae rely on the temperature, and Vass' formula additionally relies on the relative humidity [1,3,4].

Temperature increase is one of the most prominent features of anthropogenic climate change, but relative humidity is also affected [5]. These changes are very well documented, and the impacts of climate change on politics, society and the natural world are becoming increasingly well understood. The Anthropologies are an important scientific field, in which impacts of changing climate on society, medicine, and human culture are increasingly recognised, with most subfields of Anthropology now including research dedicated to climate change [6,7]. Forensic Anthropology has so far been exceptional in this regard, with almost no research into the effects climate change is likely to exert. The latter are likely to be particularly relevant to the estimation of the PMI, and therefore on forensic pathological and anthropological practice [8].

The current study presents a broad overview of the likely effects, of changing climate on the speed of decomposition, and therefore on the estimation of the PMI, in order to consider how such changes might impact the work of forensic anthropologists.

With the 2015 Paris Agreement, there is a global agreement, to limit the increase in global mean surface temperature (GMST) to a maximum of 2 °C and do everything possible to try and limit it to 1.5 °C compared

* Corresponding author.
E-mail address: mjsmith@bournemouth.ac.uk (M.J. Smith).

https://doi.org/10.1016/j.fsir.2023.100321
Received 26 January 2023; Received in revised form 4 May 2023; Accepted 20 May 2023
Available online 21 May 2023

to pre-industrial times. The social and political changes necessary to stay within those boundaries, however, have been so far slow to emerge [9,10].

The current study considers possible changes, in relation to two different climate change scenarios. The Shared Socioeconomic Pathway (SSP) scenarios are the most current summarised and published climate scenarios available at the time of writing [5]. This article considers the effects for SSP1–2.6 and SSP5–8.5 in detail. These two climate scenarios were chosen to cover a broad range of potential climate impacts. To the best knowledge of the authors, the work by Strack [8] is the only work to look into the effects of climate change on the speed of decomposition. This study utilised older climate scenarios. In order to best compare the work of this current study with the work by Strack, the SSP1–2.6 scenario was chosen over the more optimistic SSP1–1.9 scenario. The data for all other SSP scenarios are shown in the supplementary files.

As climate change is locally variable, the current study employs a strategy of averaging the effects across different climate zones, as well as across the globe. Furthermore, the effects of climate change are subject to seasonal variation, this is addressed by modelling the effects for decomposition starting in January and July [11]. To analyse the likely extent of these effects over time, projected post-mortem intervals from death to skeletonization (PMIDS) were calculated for the decades of 2020–2029 and 2090–2099.

Background

Forensic anthropology

The post mortem interval (PMI) is an important part of the forensic anthropologist's work. This is because understanding the time of death is of immense importance to the work of the police, in a crime scene investigation [2]. In consequence, estimation of the PMI has been a frequent subject for published studies in the field [1–4,12–16]. Whilst a broad set of 'stages of decomposition' was established early on [17], further research continues into what factors can affect the duration of each of these stages, and how to improve the precision of PMI estimates [1–4,12,18–21].

Amongst the many factors shown to have an effect on the duration of different stages, those generally agreed as having the greatest impact include temperature, humidity and insect activity [21].

The temperature is the single most important factor in the estimation of the PMI. In general, a higher temperature will positively correlate with the rate of chemical reactions, insect patterns, and physical changes, and will lead to a faster decomposition. Furthermore, decomposition is effectively halted if temperatures drop below 0 °C [4].

A higher humidity will also lead to faster decomposition impacting chemical reactions, as well as insect activity. A low humidity is linked to delay or cessation of decomposition and therefore natural mumification [12,13].

When accounting for different temperatures by measuring the PMI in Accumulated Degree Days (ADD), insect activity seems to have the largest impact on the speed of decomposition [21]. Increased insect activity will therefore lead to more rapid decomposition.

To account for these factors in the estimation of the PMI, multiple different methods have been developed [1,4]. Using insect activity to estimate PMI is part of the scientific field of forensic entomology, which is outside the focus of this current study [22].

Using temperature as the most important factor in decomposition, Megyesi et al. [4] developed a mathematical model to estimate the PMI more precisely. The method is based on a more detailed description of the stage of decomposition, which is achieved by a descriptive point-based system called "Total Body Score" (TBS). The TBS is determined by a visual assessment of different parts of the deceased, based on a point score described in the article by Megyesi et al. [4]. Using the TBS, a PMI in ADD can be calculated. To calculate the PMI in days, one has to divide the calculated PMI by the average temperature during decomposition. This formula is easy to use, and shows small intra- and inter observer differences. It is currently the most widely used formula to estimate the PMI, although becomes less precise with regard to the later stages of decomposition [14].

Using temperature and humidity, Vass [1] developed a formula based on data from three decades of research at the Anthropological Research Facility in Knoxville, Tennessee. Using the stage of decomposition as percentages, it is possible to calculate the PMI in days. The paper also includes a second formula for a more precise calculation when dealing with anaerobic decomposition [1]. It has been shown to be more precise than the formula by Megyesi et al., but it is still less often used [3].

Climate Change

The term climate refers to an average stage of different factors, including temperature, humidity, and wind patterns. Those factors are commonly referred to as climate factors. Even though, there is no set time period, over which the mean is calculated, most publications use the guidelines by the World Meteorological Organisation, which recommends a period of 30 years [23].

Climate change then refers to the changes of those factors across time. This does include natural changes, caused by changes in the sun's activity, or the tilt of the earth's axis, among others. Over recent years the term has come to be widely used as referring to anthropogenic climate change. This means changes in those climate factors due to human activity, such as burning coal, oil, and gas, or intensive agriculture [24,25].

Specific molecules, such as carbon dioxide, methane or water vapour, can absorb and re-emit electromagnetic radiation in the infrared spectrum. This re-emission is spherical and does not have a specific direction. This leads to an apparent reflection of infrared radiation back towards the earth's surface, which increases the overall amount of infrared radiation at the surface and creates a warming effect. As a natural process, this so-called greenhouse effect is responsible for keeping the global mean surface temperature (GMST) above 0 °C, which allows water to exist in mostly fluid form and makes life on earth possible [25].

Human activity is now adding more of those molecules, or "greenhouse gases", at a record rate. This has led to a record breaking climate change, including an unprecedented temperature increase of about 1 °C in the past 150 years, a record low ice-extent in the arctic ocean, and a rarely before seen increase of sea level, amongst other effects [26].

The Intergovernmental Panel on Climate Change was founded in the late 1980 s, to provide a summarised overview of the current state of the climate as well as future climate change scenarios [5]. In order to be able to compare models from different institutions around the world, a standardised set of social and economic parameters was developed [5]. These sets are updated regularly, with the latest set being the Shared Socioeconomic Pathway (SSP) scenarios. Five of these SSPs were used for the summary in the most recent IPCC Assessment Report. The scenarios differ in climate impact. Whilst the most optimistic scenario (SSP1–1.9) would limit the temperature increase to about 1.4 °C by 2100, compared to preindustrial times, the most pessimistic scenario (SSP5–8.5) would lead to an increase of about 4.4 °C [5].

The SSPs are clustered in 5 broader categories, relating to "scenarios following a green growth strategy (SSP1), a more middle of the road development pattern (SSP2) further fragmentation between regions (SSP3) an increase in inequality across and within regions (SSP4) and fossil fuel based economic development (SSP5)" [27]. For each of these broader categories a base line scenario was created. Based on these base line scenarios, adaptions in policy measures taken are used to incorporate more specific climate targets. These targets are measured by the expected added radiative forcing in Watts per square meter by 2100 and are adopted from the previous instalment of climate models, the Representative Concentration Pathways (RPCs). Specifically, these are

an addition of 2.6, 4.5, 6.0 and 8.5 W/m^2 [27,28]. Further policy measures based off the SSP1 base line scenario led to an improved scenario of an addition of only 1.9 W/m^2, which has been adapted as the 5th scenario for the current IPCC report [5].

In the current article, the SSP1 (specifically the SSP1–2.6) and the SSP5 (specifically the SSP5–8.5) are discussed, in order to account for a wide range of possible impacts, and comparability with existing literature (see Methods and Materials for more detail).

The SSP1 base scenario sees a slight increase in overall energy demand. This is caused by an increase in the demand for energy services due to rapid economic growth, which is mostly counteracted by improvements in efficiency. While there is a slight increase in coal use and a significant increase in natural gas consumption by mid-century, a substantial increase in renewable energy sources leads to an overall share of 65% renewables by 2100. In the agricultural sector, a global increase in food demand is seen to allow for a sustainable development and increased food availability by mid-century. Driven by a reduction of meat products in higher income countries, in combination with overall increase in efficiency and crop yield, as well as an overall population decline in the second half of the century this baseline scenario sees a decline in overall agricultural land use. This in term can be interpreted as an increase of natural land area. These changes in land use counter a slight increase in emissions from the energy sector. This SSP1 base scenario leads to an increase of ~5 W/m^2 of radiative forcing [27]. The SSP1–2.6 scenario builds on this base line scenario and incorporates active policy measures, primarily in the form of a carbon tax. This can be achieved by a comparatively low pricing that peaks in the second half of the century. Incorporating this carbon tax will mostly drive a faster decarbonisation of the energy system, leading to net negative emission in the second half of the century [27].

The unmitigated SSP5 baseline scenario is equivalent with the SSP5–8.5 scenario. The SSP5 scenario is characterised by a rapid economic growth in both high- and low-income countries, leading to an overall convergence. This convergence is also happening in the SSP1 scenario, just at about half the level compared to the SSP5. Similarly global energy demand is about twice as high in the SSP5 scenario, compared to the SSP1 scenario. In the SSP5 scenario, most of the energy demand is covered by fossil fuels. Specifically, oil consumption peaks mid-century at about twice the current amount, Natural gas consumption peaks in the second half of the century as four times the current amount and the current consumption pattern of coal is reversed to see an increase throughout the next century. Overall fossil fuel use is declining towards the end of the century. However, this is driven more by a depletion of assumed resources, rather than climate related reasons. The lack of support for renewable energy sources leads to a delayed implementation and shares start to increase only towards the end of the century. Despite a similar population development, food demand is also considerably larger in SSP5 compared to SSP1, while the reduction in animal products and food waste seen in SSP1 does not apply to the SSP5 scenario. In combination with preferable conditions for international trade, this leads to an increase in deforestation and a general expansion of agricultural land, mainly in Africa and South America. The increase in agricultural land peaks in the second half of the century. As opposed to SSP1 biomass does not play a large role in meeting the energy demand in SSP5. Overall this leads to emission-levels that are roughly three times higher in 2100 in the SSP5 compared to the SSP1. This baseline scenario leads to an addition 8.7 W/m^2 of radiative forcing and a temperature increase of 5 °C [29].

Even though the general connection between greenhouse gases (GHGs), like carbon dioxide, and the temperature has been known for a long time [30,31], there is still a wide range in the exact impacts of these greenhouse gases on the GMST. This relationship is described by the climate sensitivity of the GHGs. In climate science, this is the factor that describes the temperature response of the climate system to a doubling of the GHG, especially carbon dioxide. This factor is hard to accurately determine, as it is dependent on many different coupled factors, such as cloud coverage, that cannot yet be precisely predicted [32,33]. In the models used in the latest published IPCC report, the Coupled Model Intercomparison Project Phase 6 (CMIP 6) models, the climate sensitivity is given as a best estimate of 3 °C with a range between 2.5 and 4 °C. This is a narrower estimate than in the CMIP5 models [5]. The climate sensitivity is an important measure in the estimation of the increase of temperature. The updated climate sensitivity is partly a reason for the fast increase of temperature in the CMIP6 scenarios compared to the CMIP5 scenarios [5].

Humidity may also be impacted by changes in the GHG concentration. The term humidity is here used to refer to the relative humidity. The relative humidity cannot be easily modelled from temperature changes, and is most commonly modelled on the basis of evaporation, atmospheric circulations and dewpoint temperature. There is good overall agreement between the models and the resultant observations, which support general confidence in the modulation [34–39].

In the observational data, a slight decrease in humidity is apparent. This decrease is more prominent over land areas, than over the ocean. The temperature has been observed to increase on a global scale. This increase is more prominent towards the poles as well as over land [40].

A combination of temperature and precipitation can be used to classify different climate zones. The most commonly used classification system was developed by Köppen and further refined by Geiger. This Köppen-Geiger classification divides the land mass into five broad climate zones. This classification uses plant species as a general proxy. The first letter in the Köppen-Geiger classification specifies these broad climate zones. There are tropical (A), dry (B), temperate (C), continental (D) and polar (E), climates. The second letter in the Classification indicates the precipitation distribution, and a third letter classifies temperature distribution. The classification incorporates both annual means in precipitation and temperature, and also their distribution throughout the year [41].

The distribution of these climate zones is expected to change. Many studies have shown, these changes to have already occurred, and have modelled future changes, based on the different climate change predictions [42].

Forensic anthropology and climate

The current authors are aware of very few studies on the links between forensic anthropology and climate change. This is surprising as the importance of different climatic conditions is itself is recognised as an important factor [43]. The only studies we are aware of relating climate change to post mortem intervals are by Turchetto and Vanin [44] and Strack [8]. Turchetto and Vanin investigated changes to the distribution of forensically relevant insects. Their findings of pole-wards and upwards movement of insects is supported by findings of climate scientists [44–46]. Strack estimated the impacts that future climate change might have on the speed of decomposition. This latter project laid the groundwork for the current study which aims at addressing some of the limitations discussed by Strack and further exploring the possible future changes to the post mortem interval [8].

Methods and materials

In order to minimize biases in the climate data, the current study uses an average across four different climate models in two different scenarios. These models are the MIROC6, MRI-ESM2–0, CanESM5, and IPSL-CM6A-LR model [36–39]. The data from each of these models for the SSP scenarios are freely available through the Earth System Grid Federation (ESGF) [47–54]. The models were chosen primarily because they provide continuous monthly data for at least January 2020 to December 2099 for the temperature and relative humidity. Most models available through the ESGF do not provide datasets for relative humidity at surface level. Of the models where these datasets were available, not all models provided data for all climate scenarios, or did not provide a

continuous dataset across the abovementioned timeframe. These limitations were set to accommodate for the limited computational power available to the authors. These data are used to calculate a factor for the estimation of decomposition as $\frac{T*RH*1.03}{1285}$. In order to better establish a mean value across the different models, they are interpolated onto a 1°x1° grid using the build in interpolation formula of the xarray python package (xarray Developers 2020). As human decomposition is mostly halted below 0 °C, the formulae for PMI estimation require temperatures of above 0 °C. In the current study this is accomplished by setting all values of $\frac{T*RH*1.03}{1285}$ that are below 0–0.

The estimation of the post-mortem interval from death to skeletonization (PMIDS) is done by using the formula by Vass [1] for aerobic decomposition. We chose the formula by Vass over the formula by Megyesi et al. as it has shown to be more accurate for later stages of decomposition and shows an overall similar error rate for different climates [3,12,55]. The formula is commonly used in forensic anthropology to estimate the post mortem interval as

$$PMI = \frac{1285 * \frac{decomp}{100}}{T * RH * 0.0103},$$

with *PMI* being the post mortem interval in days, *decomp* being the loss of soft tissue in percentages, *T* being the temperature in degrees Celsius and *RH* being the relative humidity in percentages [1].

In order to calculate a PMIDS, decomposition is set to 100%. With that the formula is

$$PMIDS = \frac{1285}{T * RH * 0.0103}.$$

The temperature data, as well as the relative humidity data are available as monthly mean values from the climate models, as values for the complete atmosphere at a height of 2 m (set to be equivalent to surface values).

To estimate a PMIDS, that is reflective of temperature and humidity changes throughout the year, instead of calculating the PMIDS using seasonal averages, the decomposition is recalculated for an increasing time period until the decomposition is above 100%. Then the PMIDS is estimated through linear regression.

The PMIDS is therefore calculated as follows:

1) Calculation of the decomposition until decomposition is above 100%

$$PMI = \frac{1285 * \frac{decomp}{100}}{T * RH * 0.0103}$$

With *PMI* = post mortem interval, *decomp* = decomposition in %, *T* being the temperature and *RH* the relative humidity, then

$$PMI = decomp * \frac{1285}{T * RH * 1.03}$$

And

$$decomp = PMI * Df$$

with

$$Df = \frac{T * RH * 1.03}{1285}.$$

The decomposition is now calculated as:

$$Decomp_n = \sum_0^n PMI_n * \sum_0^n \left(Df_n * \frac{1}{n} \right)$$

With *n* being the month, for which the decomposition is calculated, $\sum_0^n (PMI)$ being the accumulated post mortem interval in days, calculated from the days of the respective month, $\sum_0^n \left(Df_n * \frac{1}{n}\right)$ being the average temperature times humidity across the respective PMI.

2) Calculation of the PMIDS

When $decomp_n$ is above 100%, the PMIDS for a decomposition of 100% is calculated by assuming a linear correlation between the last two calculated points. The PMI can now be calculated simplified as

$$PMI = F * decomp + C$$

With PMI being the post mortem interval in days, F being some factor, decomp being the decomposition in percentages and C being a constant.

The factor can now be calculated as

$$F = \frac{PMI_n - PMI_{(n-1)}}{Decomp_n - Decomp_{(n-1)}}$$

And the constant can be calculated as

$$C = PMI_n - (decomp_n * F)$$

With these information, the above formula can be rearranged to calculate the PMIDS as

$$PMIDS = F * 100 + C$$

As an example, we calculate the PMIDS, when every month is 30 days long, and each month the temperature is 15 °C and the relative humidity is 50%.

Then

$$Decomp_1 = \sum_0^1 30 * \left(\sum_0^1 \left(\frac{15 * 50 * 1.03}{1285} \right) * \frac{1}{1} \right) = 18\%$$

$$Decomp_2 = \sum_0^2 30 * \left(\sum_0^2 \left(\frac{15 * 50 * 1.03}{1285} \right) * \frac{1}{2} \right) = 36\%$$

…

$$Decomp_5 = \sum_0^5 30 * \left(\sum_0^5 \left(\frac{15 * 50 * 1.03}{1285} \right) * \frac{1}{5} \right) = 90\%$$

$$Decomp_6 = \sum_0^6 30 * \left(\sum_0^6 \left(\frac{15 * 50 * 1.03}{1285} \right) * \frac{1}{6} \right) = 108\%$$

With this,

$$F = \frac{180 - 150}{108 - 90} = 1.6667$$

And

$$C = 180 - (108 * 1.6667) = 0$$

and therefore, the PMIDS is calculated as

$$PMIDS = 1.6667 * 100 + 0 = 166.67$$

In this example, the PMIDS would be 166.67 days.

The PMIDS is only calculated for areas associated with a Köppen-Geiger classification. Thus, restricting PMIDS calculation to land-areas. Mean values are calculated for the climate zones, and a global average is calculated using area-weighting of the climate zones averages.

Antarctica was excluded from the calculations, as the continent is mostly EF-climate with no decomposition due to sub-zero-degree Celsius temperatures. This large area would have distorted the global average. Furthermore, as there is currently only a minimal population in Antarctica, the calculation of a PMIDS in that area does not have any practical importance to the topic of this research.

Of the climate zones assessed, some have a geographical distribution, that is too small for the 1°x1° grid-resolution used in this research. For the purpose of the current study, these climate zones are seen as non-existent. To account for the seasonal variability of decomposition and climate change, the PMIDS is calculated for a decomposition starting in January, and a decomposition starting in July. The complete code for this model is based on Python 3.0.1 (Python Software Foundation 2019) and is available upon request.

Results

Throughout almost all scenarios, there was a statistically significant difference ($p < 0.05$) between the PMIDS in the 2020 s and the PMIDS in the 2090 s. Notably, when there was no significant difference, it was only in some climate zones in the SSP1–2.6.

This current study looked at 29 different climate zones, as well as the overall global changes. Out of the 29 climate zones analysed, seven had a spatial resolution that was too small for the 1°x1° grid resolution. These are the Csc, Dsd, Dwa, Dwb, Dwc, Dwd, and Dfc scenarios. The Dwa scenario is excitant in the SSP5–8.5 scenario. Figs. 1 and 2.

Worldwide the decadal mean for the 2020 s was 211.11 days and 204.94 days in the SSP5–8.5 climate scenario for decomposition starting in January and July, respectively. The decadal mean for the 2020 s in the SSP1–2.6 was 212.29 days for decomposition starting in January and 207.44 days for decomposition starting in July. These decadal means shrank to 175.88 and 136.22 days in the SSP5–8.5 scenario and to 206.80 and 198.00 days in the ssp1–2.6 scenario, respectively.

When looking at the individual climate zones, the difference is statistically significant ($p < 0.05$) in most of the climate zones and scenarios. There is no statistical significance in the PMIDS between the 2020 s and 2090 s in 10 climate zones and scenarios, out of the 46 zones and scenarios (23 zones, 2 scenarios) that are analysed in this study. These were the Am (62.62 days in 2020 s, 62.23 days in 2090 s, $p = 0.483$), BWh (171.26 days, 170.03 days, $p = 1.05$), Bsh (135.41 days, 134.37 days, $p = 0.525$), Cwa (127.68 days, 126.06 days, $p = 0.117$), EF (364.45 days, 364.44 days, $p = 0.427$) climate zones in the SSP1–2.6/Summer scenario.

In the SSP1–2.6/Winter scenario the Af (56.93 days, 56.40days,

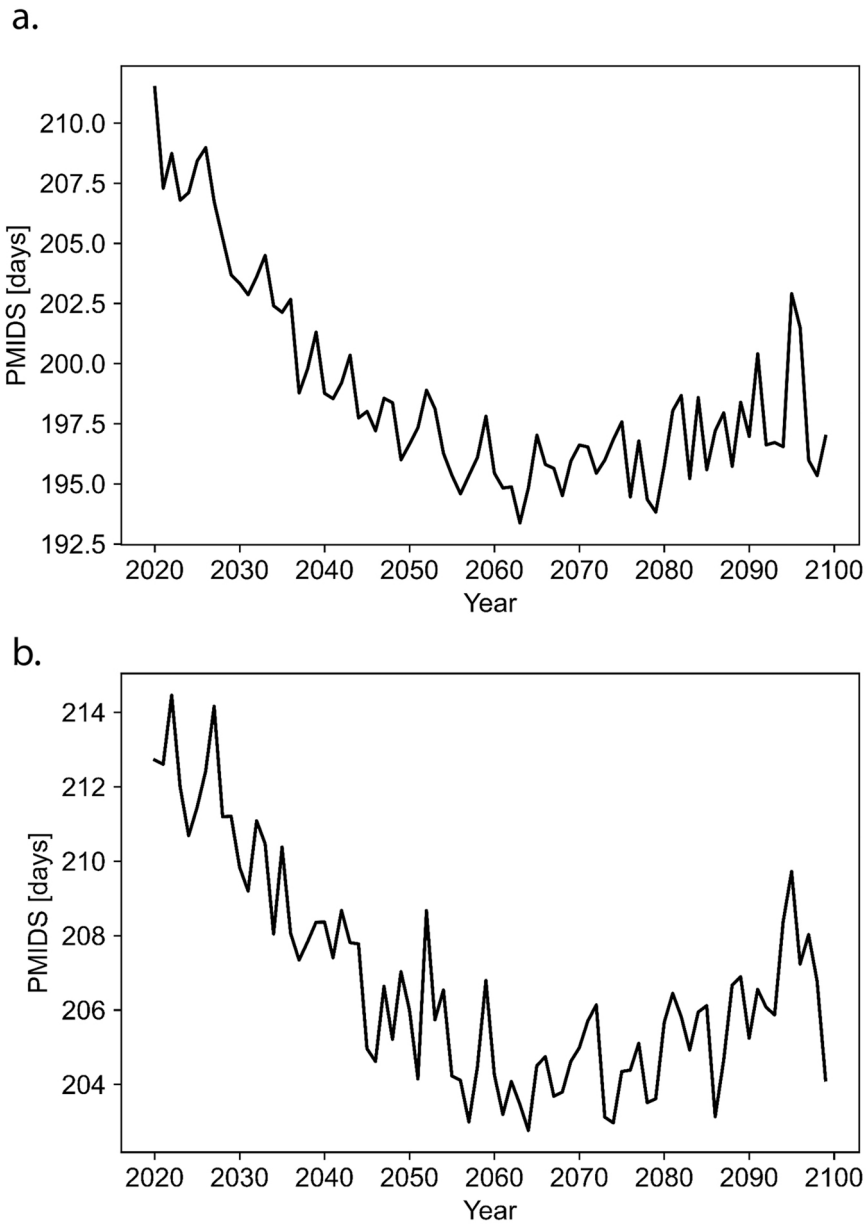

Fig. 1. Yearly Changes in PMIDS. Climate Scenario: SSP1–2.6. Comparing Decomposition starting in July (top) and January (bottom).

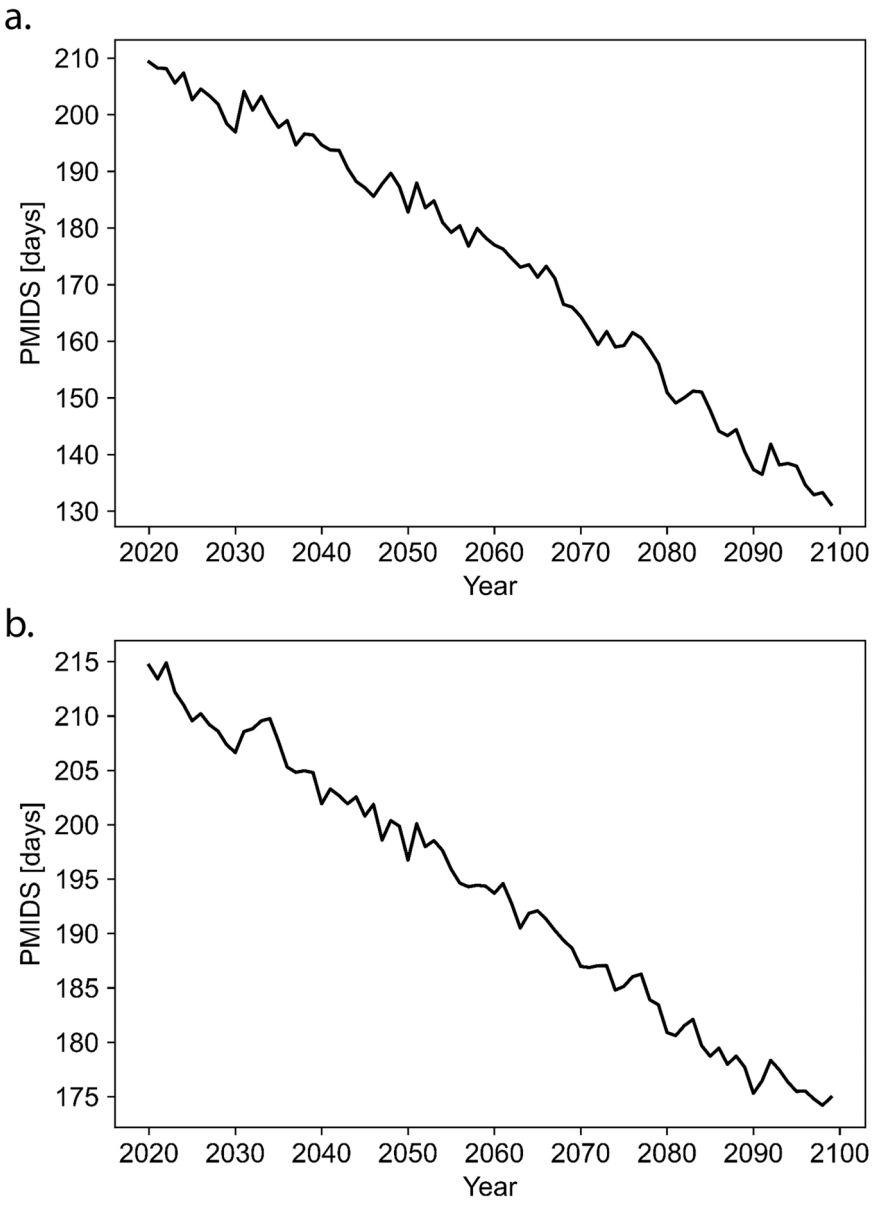

Fig. 2. Yearly Changes in PMIDS. Climate Scenario: RCP 8.5. Comparing Decomposition starting in July (top) and January (bottom).

p = 0.0758), BWh (209.86 days, 209.00 days, p = 1.39), BSh (127.65 days, 125.56 days, p = 0.0740), Cwa (74.89 days, 74.31 days, p = 0.598), and EF (364.37 days, 364.27 days, p = 0.0716) climate zones showed no significance. Tables 1 and 2 shows a list of the changes in the PMIDS for SSP1–2.6 and SSP5–8.5 for all climate zones, respectively. Figs. 3,4,5 and 6.

With decomposition starting in January, in the SSP5–8.5 scenario, the largest decrease in the PMIDS was seen in the Cwc-Climate with a 48.19% decrease between the 2020 s and 2090 s. The lowest decrease was seen in the ET-Climate, where the PMIDS decreased by 0.22%. With decomposition starting in July, in the RCP 8.5 scenario, the largest decrease was in the Dfd-Climate with 60.86% between the 2020 s and 2090 s. This is also the largest decrease across all scenarios. The lowest decrease was again in the EF-Climate with 0.30%.

In the SSP1–2.6 scenario, with decomposition starting in January, the largest decrease could be seen in the Cwc-Climate with 8.50% and the lowest decrease was in the EF-Climate with 0.03% (not statistically significant, p = 0.07). With decomposition starting in July, the largest decrease was 18.81% in the Dfd-Climate. In the ET-Climate nearly no change (−0.0016%) was detected. This change was not significant.

Discussion

Limitations of the climate data

To reduce the biases in the climate data, the mean value across four different models was calculated. This reduces the biases from individual models, however, there are still some general limitations to the climate data, that should be mentioned. While there are no extensive studies, the authors are aware of, that look into the prediction of the relative humidity itself, many look into the modulation of the precipitation. This precipitation bias is used as a general indicator for the relative humidity, even though, this is not a perfect substitute. Looking into temperature and precipitation, all models seem to have a smaller bias for the northern hemisphere than for the southern hemisphere, and all models seem to have a smaller bias during the months of December, January, and February (DJF), than during the months of June, July, and August (JJA). In general, the temperature, seems to have a positive bias, which correlates to a negative bias in the precipitation, as well as in the relative humidity, judging from the few individual models, that had a separate analysis for the bias in the relative humidity [56]. The selection of the

Table 1
Changes in the PMIDS for a global average and the different climate zones. Climate scenario: SSP5–8.5. Note the highest decrease and the lowest decrease (marked as in bold/italics).

Climate Zone	PMIDS, 2020–2029, Winter	PMIDS, 2090–2099, Winter	Diff. [%]	p-value	PMIDS, 2020–2029, Summer	PMIDS, 2090–2099, Summer	Diff. [%]	p-value
Global	211.11	175.88	-16.69	1.88E-18	204.94	136.22	-33.53	7.37E-20
Af	57.15	51.62	-9.68	8.64E-13	56.22	50.80	-9.65	1.37E-10
Am	66.27	60.92	-8.06	1.07E-11	62.53	58.65	-6.21	1.95E-06
Aw	74.76	67.72	-9.41	6.35E-16	84.45	80.11	-5.14	4.87E-11
BWh	208.99	187.23	-10.41	8.40E-10	170.97	138.09	-19.23	8.92E-14
BWk	312.53	242.06	-22.55	3.19E-17	329.54	256.59	-22.14	6.65E-14
BSh	128.70	112.80	-12.36	1.93E-12	137.30	123.40	-10.13	1.47E-12
BSk	252.29	201.36	-20.19	4.54E-15	279.86	200.35	-28.41	6.27E-15
Csa	177.83	150.68	-15.27	5.99E-13	124.60	100.44	-19.39	2.53E-12
Csb	171.05	139.74	-18.31	1.44E-12	108.38	80.89	-25.37	5.19E-13
Cwa	75.03	66.46	-11.43	2.25E-12	124.26	114.62	-7.76	8.02E-12
Cwb	135.21	92.94	-31.26	1.38E-17	169.08	138.61	-18.02	5.49E-17
Cwc	202.60	104.96	***-48.19***	2.24E-18	209.28	138.87	-33.64	6.08E-15
Cfa	133.72	113.67	-14.99	3.40E-16	85.36	75.81	-11.18	1.65E-11
Cfb	175.98	136.59	-22.38	2.23E-18	129.15	104.81	-18.85	1.06E-15
Cfc	263.68	157.73	-40.18	1.89E-18	249.50	176.70	-29.18	1.65E-17
Das	244.88	199.49	-18.54	5.88E-13	260.68	162.82	-37.54	1.37E-15
Dsb	267.74	214.96	-19.71	1.23E-15	292.39	159.14	-45.57	2.27E-20
Dsc	343.59	235.16	-31.56	7.78E-21	362.28	171.60	-52.63	6.51E-20
Dwa	204.21	185.92	-8.95	1.41E-11	73.75	57.73	-21.72	4.53E-11
Dfa	213.04	185.98	-12.70	3.86E-15	150.48	85.54	-43.16	1.74E-14
Dfb	236.18	201.64	-14.63	6.63E-16	220.18	86.17	***-60.86***	6.61E-17
Dfc	321.01	232.98	-27.42	2.36E-18	353.88	169.21	-52.18	1.75E-18
ET	362.01	336.20	-7.13	9.48E-16	362.34	328.97	-9.21	4.38E-14
EF	364.27	363.49	***-0.22***	2.11E-12	364.43	363.34	***-0.30***	7.88E-08

models is mostly based on the selection of available datasets, which provided a continuous dataset for both relative humidity and temperature at a surface level as a monthly mean for the January 2020 to December 2099 timeframe. Some biases might be further reduced by incorporating datasets which require a more extensive pre-processing.

Limitations of the post-mortem interval calculation

The post-mortem interval formula used in this current study to calculate the post-mortem interval from death until skeletonization (PMIDS) has been tested in multiple different locations, with different climate. These validation studies concluded, that the formula is not accurately predicting the PMI in climate zones outside of Knoxville, Tennessee, where it was developed. More specifically, drier and colder climates seem to lead to a wrongful estimation, especially in later stages of decomposition. Therefore, it is likely that the estimations in different climate zones may present an unknown bias [3,12]. Current literature comparing the formulae by Vass and Megyesi et al. show a wrongful estimation of the PMI in drier and colder climates for both. Overall the formula by Megyesi et al. seems to show a greater deviation from the real PMI for later stages of the decomposition, compared to the formula by Vass [3,12,55].

Overall assessment of the results

Overall, the results are consistent with what was expected from the current literature on climate change. In general, it was expected, that there is an overall lower decline in the PMIDS in the SSP1–2.6 scenario, compared to the SSP5–8.5 scenario. Furthermore, the general trend visible in the results is that the climate zones of the tropical climate, the A-climates, are the least affected, and that the C/D Climates are more affected, are in accordance to climate research. Due to multiple effects, regions closer to the poles, are warming faster than the regions closer to the tropics. Changes in temperature are overall more prominent than changes in the relative humidity. Therefore, these effects of the temperature changes are more prominently influencing the PMIDS

Table 2
Changes in the PMIDS for a global average and the different climate zones. Climate scenario: SSPP1–2.6. Note the highest decrease and the lowest decrease (in bold and Italics). Also note the cells marked bold where no significant change happens.

	PMIDS, 2020–2029, Winter	PMIDS, 2090–2099, Winter	Diff. [%]	p-value	PMIDS, 2020–2029, Summer	PMIDS, 2090–2099, Summer	Diff. [%]	p-value
Global	212.29	206.80	-2.59	2.23E-07	207.44	198.00	-4.55	1.11E-07
Af	56.93	56.40	-0.94	**7.58E-02**	56.24	55.34	-1.61	4.87E-05
Am	65.89	65.08	-1.22	4.68E-02	62.62	62.23	-0.62	**4.83E-01**
Aw	74.98	74.22	-1.02	2.66E-02	84.64	83.89	-0.88	1.32E-03
BWh	209.86	209.00	-0.41	**1.39E+ 00**	171.26	170.03	-0.72	**1.05E+ 00**
BWk	313.31	305.82	-2.39	1.33E-02	327.76	322.31	-1.66	1.50E-02
BSh	127.65	125.56	-1.64	**7.40E-02**	135.41	134.37	-0.76	**5.25E-01**
BSk	252.83	246.33	-2.57	3.08E-02	277.34	267.61	-3.51	1.52E-03
Csa	178.09	172.68	-3.04	5.72E-03	124.69	120.74	-3.17	2.21E-02
Csb	175.38	169.18	-3.54	3.35E-03	111.33	104.12	-6.48	1.87E-03
Cwa	74.89	74.31	-0.77	**5.98E-01**	127.68	126.06	-1.27	**1.17E-01**
Cwb	133.21	126.39	-5.12	1.98E-04	167.17	162.42	-2.84	8.73E-06
Cwc	214.26	196.06	***-8.49***	2.92E-04	220.17	204.39	-7.17	7.29E-05
Cfa	132.51	129.38	-2.36	4.92E-06	85.38	83.44	-2.28	1.32E-06
Cfb	174.44	169.05	-3.09	1.93E-05	128.29	123.69	-3.59	9.26E-05
Cfc	263.15	250.94	-4.64	1.88E-02	250.73	238.42	-4.91	6.53E-03
Das	248.47	240.35	-3.27	8.79E-03	265.46	252.23	-4.98	1.85E-02
Dsb	272.59	263.34	-3.39	8.13E-03	300.59	272.35	-9.39	3.72E-07
Dsc	343.38	328.03	-4.47	3.78E-05	362.23	357.96	-1.18	1.48E-03
Dfa	212.88	209.02	-1.81	1.48E-05	152.42	134.46	-11.78	3.65E-05
Dfb	235.59	228.73	-2.91	8.45E-08	223.74	181.65	***-18.81***	9.37E-09
Dfc	320.81	304.23	-5.17	7.99E-11	355.06	341.56	-3.80	1.37E-07
ET	361.84	360.67	-0.32	1.02E-05	362.21	361.40	-0.22	7.56E-07
EF	364.37	364.27	***-0.03***	**7.16E-02**	364.45	364.44	***0.00***	**4.27E-01**

calculation, than the changes in humidity.

The E-Climate, which are defined by their number of days below zero, show a smaller difference in the modelled PMIDS, than the D or C climate, even though the E-Climates are warming faster than the C/D Climates. This apparent discrepancy between the climate change prediction and the PMIDS modulation can be explained by the way human decomposition works. In general, human decomposition is thought to be halted if temperatures drop below 0 °C. At the very least it is slowed down extensively. Therefore, if the temperature of a region is below zero degrees Celsius, the model used in this current study will not advance the decomposition. This leads to a cut-off point, where even a large increase in temperature will not be mirrored in the PMIDS, if the temperature continues to stay below 0 °C. Secondly, PMIDS modulation is cut off at 365 days. This means, that any decomposition, that would take longer than 365 days (or one year) is going to be cut off and set to 365 days. This cut off points means, that even areas with some above-zero months, will be cut off. This threshold temperature is further contributing to a smaller difference in the E-climates, than expected from just the changes in temperature. This is again, because even a large increase in temperature may not be mirrored in that extent, if that increase does not fully happen above this threshold temperatures. For example, a change in temperature from − 20–0 °C may be a temperature increase of 20 °C, but will not result in any changes of the PMIDS, as there is still no composition calculated at 0 °C.

Comparison of the results to previous work

In the preliminary study [8] the PMIDS was calculated via a seasonal mean value, as opposed to the more direct calculation assumed in the current study. Furthermore, the values for temperature and the relative humidity included values from both, land and ocean areas. As noted in the discussion of that master thesis the ocean is functioning as a heat storage, and has a buffering function. Furthermore, the comparison in the master thesis was done for continents, not for climate zones. Lastly, the master thesis used the RCP SSPs [8].

Despite these differences, a comparison of the results for the global averages shows similar results. First of all, the results only differ by a few percentages, but have the same order of magnitude. In the RCP 8.5/ SSP5–8.5 scenario, this current study shows a higher increase in speed of decomposition. While the increase in speed of decomposition was 27.5% in JJA in the previous study [8], it is 33.5% for decomposition starting in July in this current study. For the DJF/decomposition starting in January, the increase was 12.6% in the master thesis and is 16.7% in the current study[8].

In RCP2.6/ SSP1–2.6 the differences between the two studies are smaller. For JJA/decomposition starting in July, the decrease in PMIDS was 5.2% in the preliminary project [8] as opposed to 4.6% in the current study. For DJF/decomposition starting in January it is 2.7% in the previous study and 2.6% in this current study [8]. These differences are easily explained by the different methodological approaches and the updated Climate data used. Most of the difference between the DJF/JJA values can be explained through the mean values used in the prior study, as these would lead to a slower decomposition in DJF and a faster decomposition in JJA, as opposed to the continuous calculation used in the current study. The overall higher rates of changes in the SSP5–8.5 climate scenario in this current study are likely a results of restricting calculation to the land areas, as changes in temperature and humidity are more prominent on land than on ocean [8,26], as well as the usage of the updated climate modelling data, which shows a generally faster increase in temperature [5,57].

It should be noted, that the increase in the speed of decomposition, especially in colder climate zones may be directly impacting the work of the forensic anthropologist. The PMIDS calculated in the current study can also be seen as a proxy for environmental conditions. The decrease in the PMIDS is more severe in climate zones, that mirror environmental conditions, in which the most commonly used formulas for PMI estimation are working accurately. This decrease on the PMIDS is mirroring a shift in environmental conditions towards conditions, where these formulae are currently less accurate. Therefore, climate change, especially in the SSP585 scenario, may negatively impact the accuracy of PMI estimation.

Furthermore, an increase in the speed of decomposition may lead to a higher workload for forensic anthropologists. This is because faster decomposition will decrease the time needed for a corpse to skeletonize and for the expertise of forensic anthropologists to be needed.

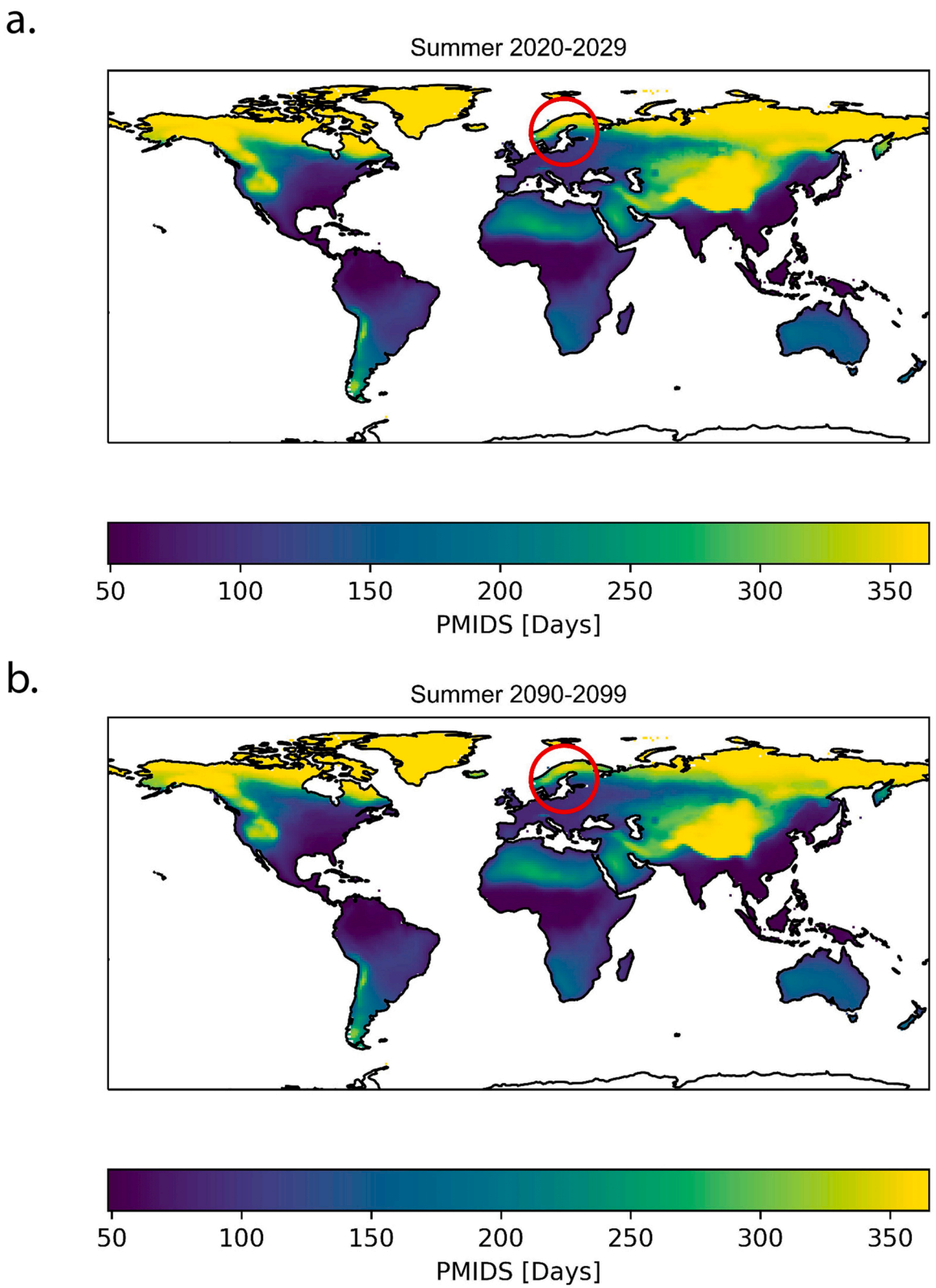

Fig. 3. Spatial variation in PMIDS. Scenario: SSP1–2.6, decomposition starting in July. Note the minimal changes, most visible when comparing areas marked with the red circle. 2020 s are at the top, 2090 s at the bottom.

Conclusion

The current study shows that climate change is exerting multiple impacts on the estimation of the post-mortem interval (PMI). Specifically, there are two main factors to consider. Firstly, the estimation of the PMI in the current study is based on the formula by Vass, which is a widely used, and currently regarded as the most accurate formula for estimating the PMI on a global scale. It is however important to note, that this formula is not accurately estimating the PMI in colder and drier climates. Looking at the PMI, it is obvious, that many places in the world

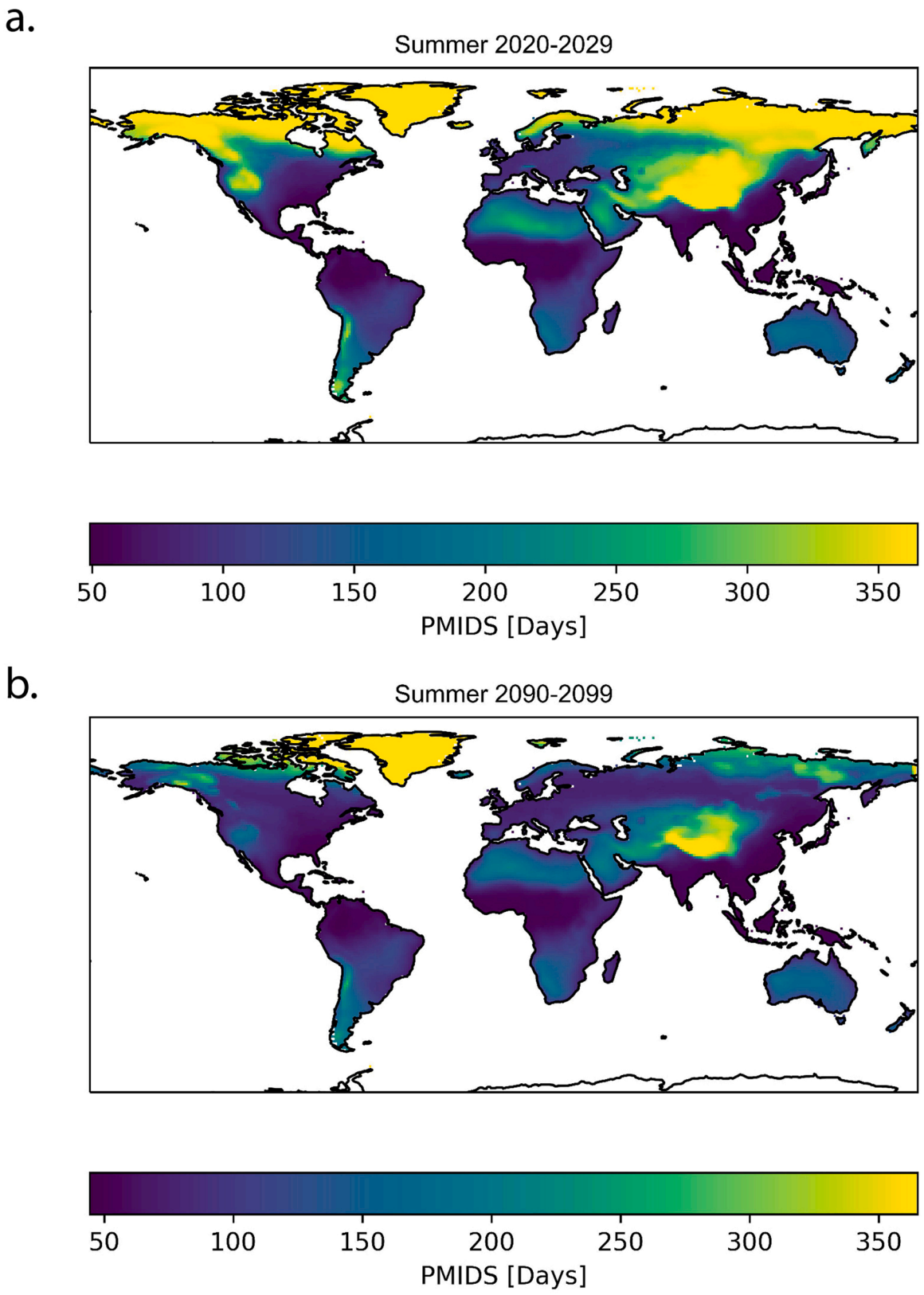

Fig. 4. Spatial variation in PMIDS. Scenario: SSP5–8.5, decomposition starting in July. Note the extensive changes, especially visible in the northern hemisphere. Top: 2020 s, bottom: 2090 s.

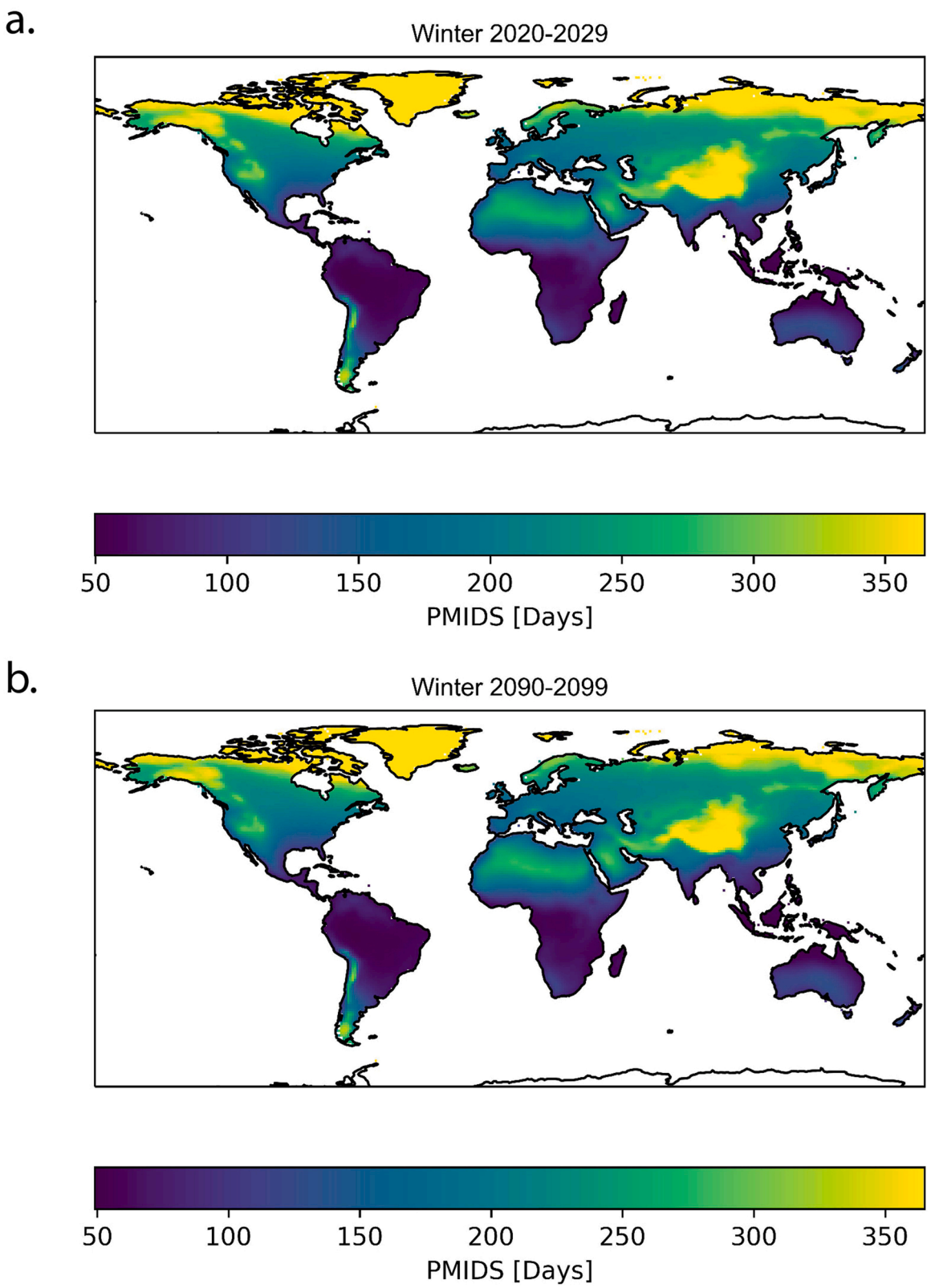

Fig. 5. Spatial variation in PMIDS. Scenario: SSP1–2.6, decomposition starting in January. Note the minimal changes, most visible when comparing areas marked with the red circle. Top: 2020 s, bottom: 2090 s.

already are less accurately represented by this formula. The formula has been developed with data from Tennessee alone and may therefore be less precise when applied to other regions, particularly those where the climate reaches the greatest extremes such as parts of Africa and Australasia. The expected climatic changes, as shown in this paper, will lead to an extension of the area, where the formulae currently used for PMI estimation become less accurate. The current authors therefore recommend that more research should focus on developing a PMI-

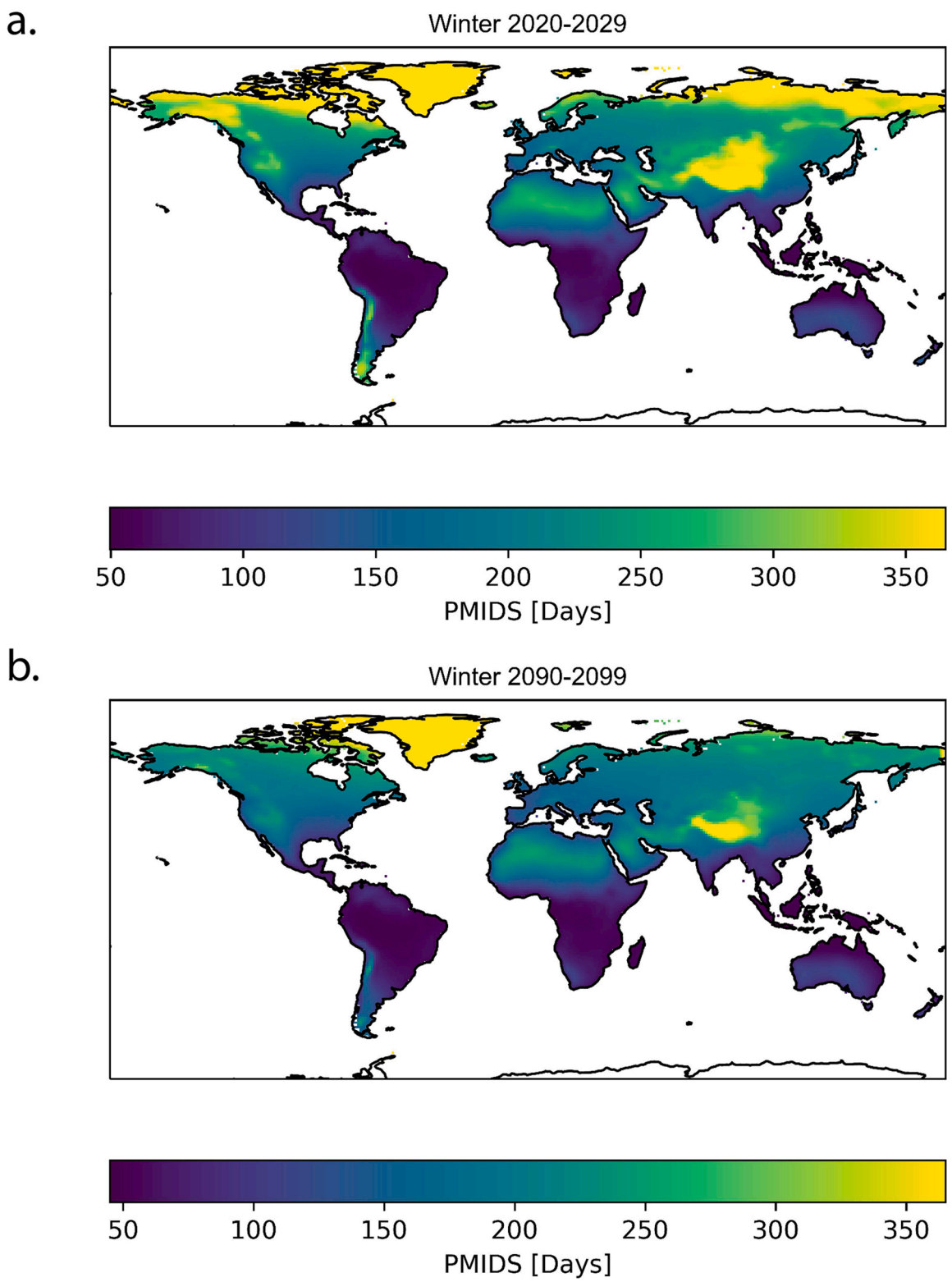

Fig. 6. Spatial variation in PMIDS. Scenario: SSP5–8.5 decomposition starting in January. Note the extensive changes, especially visible in the northern hemisphere. Top: 2020 s, bottom: 2090 s.

formula that is more accurate in estimating the PMI in drier and warmer climates. This can be achieved by strengthening the research effort in different climatic conditions outside of the United States, which provide a closer approximation of expected future climates, especially under the SSP5–8.5 climate scenario.

The current article does not purport to give an exact projection of the current state of decomposition, or future changes. Instead, the results presented here show, that the impact of climate change on the post mortem interval estimation, has long been underestimated. It is recommended, to further explore these impacts, including through incorporation of further revised climate predictions, alternative PMI – estimation formulae and the impacts that climate change may have on

buried bodies.

Declaration of Competing Interest

No conflicts of interest declared in relation to the submitted study.

Appendix A. Supporting information

Supplementary data associated with this article can be found in the online version at doi:10.1016/j.fsir.2023.100321.

References

[1] A.A. Vass, The elusive universal post-mortem interval formula, Forensic Sci. Int. 204 (2011) 34–40, https://doi.org/10.1016/j.forsciint.2010.04.052.

[2] M.T. Ferreira, E. Cunha, Can we infer post mortem interval on the basis of decomposition rate? A case from a Portuguese cemetery, Forensic Sci. Int. 226 (2013) 298.e1–298.e6, https://doi.org/10.1016/j.forsciint.2013.01.006.

[3] S.J. Marhoff-Beard, S.L. Forbes, H. Green, The validation of 'universal' PMI methods for the estimation of time since death in temperate Australian climates, Forensic Sci. Int. 291 (2018) 158–166, https://doi.org/10.1016/j.forsciint.2018.08.022.

[4] M.S. Megyesi, S.P. Nawrocki, N.H. Haskell, Using accumulated degree-days to estimate the postmortem interval from decomposed human remains, J. Forensic Sci. 50 (2005) 1–9, https://doi.org/10.1520/jfs2004017.

[5] Climate Change 2021: The Physical Science Basis. Contribution of Working Group I to the Sixth Assessment Report of the Intergovernmental Panel on Climate Change, Cambridge University Press, Cambridge, United Kingdom und New York, NY, USA, n.d. https://doi.org/10.1017/9781009157896.

[6] S. Dalsgaard, The commensurability of carbon: making value and money of climate change, HAU: J. Ethnogr. Theory 3 (2013) 80–98, https://doi.org/10.14318/hau3.1.006.

[7] J. Barnes, M. Dove, M. Lahsen, A. Mathews, P. McElwee, R. McIntosh, F. Moore, J. O'Reilly, B. Orlove, R. Puri, H. Weiss, K. Yager, Contribution of anthropology to the study of climate change, Nat. Clim. Change 3 (2013) 541–544, https://doi.org/10.1038/nclimate1775.

[8] J.B. Strack, The effects of climate change on the speed of decomposition, MSc. Thesis (2020), https://doi.org/10.13140/RG.2.2.12769.84324/1.

[9] UN, Paris Agreement, United Nations, 2015.

[10] V. Masson-Delmotte, P. Zhai, H.-O. Pörtner, D. Roberts, J. Skea, P.R. Shukla, A. Pirani, W. Moufouma-Okia, C. Pean, R. Pidcock, S. Connors, J.B.R. Matthews, Y. Chen, X. Zhou, M.I. Gomis, E. Lonnoy, T. Maycock, M. Tignor, T. Waterfield, Global Warming of 1.5°C. An IPCC Special Report in the impacts of global warming of 1.5°C above the pre-industrial levels and related global greenhouse gas emission pathways, in the context of strengthening the global response to the threath of climate ch, 2018.

[11] J. Kreyling, K. Grant, V. Hammerl, M.A.S. Arfin-Khan, A.V. Malyshev, J. Peñuelas, K. Pritsch, J. Sardans, M. Schloter, J. Schuerings, A. Jentsch, C. Beierkuhnlein, Winter warming is ecologically more relevant than summer warming in a cool-temperate grassland, Sci. Rep. 9 (2019) 1–9, https://doi.org/10.1038/s41598-019-51221-w.

[12] D.L. Cockle, L.S. Bell, Human decomposition and the reliability of a "Universal" model for post mortem interval estimations, Forensic Sci. Int. 253 (2015) 136.e1–136.e9, https://doi.org/10.1016/j.forsciint.2015.05.018.

[13] T.H. Chua, Use Temp. Model Estim. Post. Interval Forensic Entomol. (2014).

[14] M.N.S. Forbes, D.A. Finaughty, K.L. Miles, V.E. Gibbon, Inaccuracy of accumulated degree day models for estimating terrestrial post-mortem intervals in Cape Town, South Africa, Forensic Sci. Int. 296 (2019) 67–73, https://doi.org/10.1016/j.forsciint.2019.01.008.

[15] A. Baptista, M. Pedrosa, F. Curate, M.T. Ferreira, M.P.M. Marques, Estimation of the post-mortem interval in human bones by infrared spectroscopy, Int J. Leg. Med 136 (2022) 309–317, https://doi.org/10.1007/s00414-021-02641-9.

[16] G. Falgayrac, R. Vitale, Y. Delannoy, H. Behal, G. Penel, L. Duponchel, T. Colard, Critical aspects of Raman spectroscopy as a tool for postmortem interval estimation, Talanta 249 (2022), 123589, https://doi.org/10.1016/j.talanta.2022.123589.

[17] W.C. Rodriguez, W.M. Bass, Insect activity and its relationship to decay rates of human cadavers in east tennessee, J. Forensic Sci. 28 (1983) 423–432.

[18] L.G. Roberts, J.R. Spencer, G.R. Dabbs, The effect of body mass on outdoor adult human decomposition, J. Forensic Sci. 62 (2017) 1145–1150, https://doi.org/10.1111/1556-4029.13398.

[19] A. Spicka, R. Johnson, J. Bushing, L.G. Higley, D.O. Carter, Carcass mass can influence rate of decomposition and release of ninhydrin-reactive nitrogen into gravesoil, Forensic Sci. Int. 209 (2011) 80–85, https://doi.org/10.1016/j.forsciint.2011.01.002.

[20] E.M.J. Schotsmans, W. Van de Voorde, J. De Winne, A.S. Wilson, The impact of shallow burial on differential decomposition to the body: a temperate case study, Forensic Sci. Int. 206 (2011) e43–e48, https://doi.org/10.1016/j.forsciint.2010.07.036.

[21] T. Simmons, R.E. Adlam, C. Moffatt, Debugging decomposition data - comparative taphonomic studies and the influence of insects and carcass size on decomposition rate, J. Forensic Sci. 55 (2010) 8–13, https://doi.org/10.1111/j.1556-4029.2009.01206.x.

[22] A. Röglin, C.A. Szentiks, J. Dreßler, B. Ondruschka, M. Schwarz, Entomological identification of the post-mortem colonization of wolf cadavers in different decomposition stages, Sci. Justice 62 (2022) 520–529, https://doi.org/10.1016/j.scijus.2022.07.004.

[23] WMO, Guide to Climatological Practices, World Meteorological Institution, Geneva, 2018.

[24] A. Anderson, Media, politics and climate change: towards a new research agenda, Sociol. Compass 3 (2009) 166–182, https://doi.org/10.1111/j.1751-9020.2008.00188.x.

[25] N. Cubasch, U. Wuebbles, D. Chen, D. Facchini, M.C. Frame, D. Mahowald, J.-G. Winther, in: T. Stocker, T.F. Qin, D. Plattner, G.-K., P.M. M., S.K. Allen, J. Boschung, A. Nauels, Y. Xia, V. Bex, Midgley (Eds.), The Physical Science Basis. Contribution of Working Group I to the Fifth Assessment Report of the Intergovernmental Panel on Climate Change, Cambridge University Press, Cambridge, 2013.

[26] M.R. Allen, O.P. Dube, W. Solecki, F. Aragón-Durand, W. Cramer, S. Humphreys, M. Kainuma, J. Kala, N. Mahowald, Y. Mulugetta, R. Perez, M. Wairiu, K. Zickfeld, Framing and Conetxt, in: V. Masson-Delmotte, P. Zhai, H.-O. Pörtner, D. Roberts, J. Skea, P.R. Shukla, A. Pirani, W. Moufouma-Okia, C. Péan, R. Pidcock, S. Connors, J.B.R. Matthews, Y. Chen, X. Zhou, M.I. Gomis, E. Lonnoy, T. Maycock, M. Tignor, T. Waterfield (Eds.), Glob. Warm. 1. 5°C. IPCC Spec. Rep. Impacts Glob. Warm. 1. 5°C Pre-Ind. Lev. Amd Relat. Glob. Greenh. Gas. Emiss. Pathw., Context Strengething Glob. Response Threat Clim. Change (2018).

[27] D.P. Van Vuuren, E. Stehfest, D.E.H.J. Gernaat, J.C. Doelman, M. Van Den Berg, M. Harmsen, H.S. De Boer, L.F. Bouwman, V. Daioglou, O.Y. Edelenbosch, B. Girod, T. Kram, L. Lassaletta, P.L. Lucas, H. Van Meijl, C. Müller, B.J. Van Ruijven, S. Van Der Sluis, A. Tabeau, Energy, land-use and greenhouse gas emissions trajectories under a green growth paradigm, in: Global Environmental Change, 42, 2017, pp. 237–250, https://doi.org/10.1016/j.gloenvcha.2016.05.008.

[28] D.P. Van Vuuren, E. Kriegler, B.C. O'Neill, K.L. Ebi, K. Riahi, T.R. Carter, J. Edmonds, S. Hallegatte, T. Kram, R. Mathur, H. Winkler, A new scenario framework for Climate Change Research: scenario matrix architecture, Clim. Change 122 (2014) 373–386, https://doi.org/10.1007/s10584-013-0906-1.

[29] E. Kriegler, N. Bauer, A. Popp, F. Humpenöder, M. Leimbach, J. Strefler, L. Baumstark, B.L. Bodirsky, J. Hilaire, D. Klein, I. Mouratiadou, I. Weindl, C. Bertram, J.-P. Dietrich, G. Luderer, M. Pehl, R. Pietzcker, F. Piontek, H. Lotze-Campen, A. Biewald, M. Bonsch, A. Giannousakis, U. Kreidenweis, C. Müller, S. Rolinski, A. Schultes, J. Schwanitz, M. Stevanovic, K. Calvin, J. Emmerling, S. Fujimori, O. Edenhofer, Fossil-fueled development (SSP5): An energy and resource intensive scenario for the 21st century, Glob. Environ. Change 42 (2017) 297–315, https://doi.org/10.1016/j.gloenvcha.2016.05.015.

[30] S. Arrhenius, XXXI. On the influence of carbonic acid in the air upon the temperature of the ground, Lond.,Edinb., Dublin Philos. Maganzine J. Sci. 41 (1896) 237–276, https://doi.org/10.1080/14786449608620846.

[31] E. Foote, Circumstances affecting the heat of the sun's rays, The American Journal of Science and Arts. 22 (n.d.) 383–384.

[32] J.T. Kiehl, Twentieth century climate model response and climate sensitivity, Geophys. Res. Lett. 34 (2007) 1–4, https://doi.org/10.1029/2007GL031383.

[33] M.D. Zelinka, T.A. Myers, D.T. McCoy, S. Po-Chedley, P.M. Caldwell, P. Ceppi, S. A. Klein, K.E. Taylor, Causes of higher climate sensitivity in CMIP6 models, Geophys. Res. Lett. 47 (2020) 1–12, https://doi.org/10.1029/2019GL085782.

[34] E. Eccel, Estimating air humidity from temperature and precipitation measures for moddeling applications, Meteorol. Appl. 19 (2012) 118–128.

[35] S.C. Sheerwood, W. Ingram, Y. Tsushima, M. Satoh, M. Roberts, P.L. Vidale, P. A. O'Gorman, Relative humidity changes in a warmer climate, J. Geophys. Res. 115 (2010), https://doi.org/10.1029/2009JD012585.

[36] H. Tatebe, T. Ogura, T. Nitta, Y. Komuro, K. Ogochi, T. Takemura, K. Sudo, M. Sekiguchi, M. Abe, F. Saito, M. Chikira, S. Watanabe, M. Mori, N. Hirota, Y. Kawatani, T. Mochizuki, K. Yoshimura, K. Takata, R. O'ishi, D. Yamazaki, T. Suzuki, M. Kurogi, T. Kataoka, M. Watanabe, M. Kimoto, Description and basic evaluation of simulated mean state, internal variability, and climate sensitivity in MIROC6, Geosci. Model Dev. 12 (2019) 2727–2765, https://doi.org/10.5194/gmd-12-2727-2019.

[37] N.C. Swart, J.N.S. Cole, V.V. Kharin, M. Lazare, J.F. Scinocca, N.P. Gillett, J. Anstey, V. Arora, J.R. Christian, S. Hanna, Y. Jiao, W.G. Lee, F. Majaess, O. A. Saenko, C. Seiler, C. Seinen, A. Shao, L. Solheim, K. von Salzen, D. Yang, B. Winter, The Canadian earth system model version 5 (CanESM5.0.3), Clim. Earth Syst. Model. (2019), https://doi.org/10.5194/gmd-2019-177.

[38] S. Yukimoto, H. Kawai, T. Koshiro, N. Oshima, K. Yoshida, S. Urakawa, H. Tsujino, M. Deushi, T. Tanaka, M. Hosaka, S. Yabu, H. Yoshimura, E. Shindo, R. Mizuta, A. Obata, Y. Adachi, M. Ishii, The meteorological research institute earth system model version 2.0, MRI-ESM2.0: description and basic evaluation of the physical component, J. Meteorol. Soc. Jpn. 97 (2019) 931–965, https://doi.org/10.2151/jmsj.2019-051.

[39] O. Boucher, J. Servonnat, A.L. Albright, O. Aumont, Y. Balkanski, V. Bastrikov, S. Bekki, R. Bonnet, S. Bony, L. Bopp, P. Braconnot, P. Brockmann, P. Cadule, A. Caubel, F. Cheruy, F. Codron, A. Cozic, D. Cugnet, F. D'Andrea, P. Davini, C. de Lavergne, S. Denvil, J. Deshayes, M. Devilliers, A. Ducharne, J.-L. Dufresne, E. Dupont, C. Éthé, L. Fairhead, L. Falletti, S. Flavoni, M.-A. Foujols, S. Gardoll, G. Gastineau, J. Ghattas, J.-Y. Grandpeix, B. Guenet, E. Guez Lionel, E. Guilyardi, M. Guimberteau, D. Hauglustaine, F. Hourdin, A. Idelkadi, S. Joussaume, M. Kageyama, M. Khodri, G. Krinner, N. Lebas, G. Levavasseur, C. Lévy, L. Li, F. Lott, T. Lurton, S. Luyssaert, G. Madec, J.-B. Madeleine, F. Maignan, M. Marchand, O. Marti, L. Mellul, Y. Meurdesoif, J. Mignot, I. Musat, C. Ottlé,

P. Peylin, Y. Planton, J. Polcher, C. Rio, N. Rochetin, C. Rousset, P. Sepulchre, A. Sima, D. Swingedouw, R. Thiéblemont, A.K. Traore, M. Vancoppenolle, J. Vial, J. Vialard, N. Viovy, N. Vuichard, Presentation and evaluation of the IPSL-CM6A-LR climate model, J. Adv. Model. Earth Syst. 12 (2020), e2019MS002010, https://doi.org/10.1029/2019MS002010.

[40] M.P. Byrne, P.A. O'Gorman, Link between land-ocean warming contrast and surface relative humidities in simulations with coupled climate models, Geophys. Res. Lett. 40 (2013) 5223–5227, https://doi.org/10.1002/grl.50971.

[41] W. Köppen, R. Geiger, Wandkarte: Klima der, Erde, Darmstadt (1954).

[42] I. Mahlstein, J.S. Daniel, S. Solomon, Pace of shifts in climate regions increases with global temperature, Nat. Clim. Change 2 (2013) 739–743, https://doi.org/10.1038/nclimate1876.

[43] J. Meyer, B. Anderson, D.O. Carter, Seasonal variation of carcass decomposition and gravesoil chemistry in a cold (Dfa) climate, J. Forensic Sci. 58 (2013) 1175–1182, https://doi.org/10.1111/1556-4029.12169.

[44] M. Turchetto, S. Vanin, Forensic entomology and climatic change, Forensic Sci. Int. 146 (2004) 207–209, https://doi.org/10.1016/j.forsciint.2004.09.064.

[45] J.K. Hill, C.D. Thomas, B. Huntley, Climate and habitat availability determine 20th century changes in a butterfly's range margin, Proc. R. Soc. B: Biol. Sci. 266 (1999) 1197–1206, https://doi.org/10.1098/rspb.1999.0763.

[46] D.S. Pureswaran, A. Roques, A. Battisti, Forest insects and climate change, Curr. For. Rep. 4 (2018) 35–50, https://doi.org/10.1007/s40725-018-0075-6.

[47] H. Shiogama, M. Abe, H. Tatebe, MIROC MIROC6 model output prepared for CMIP6 ScenarioMIP ssp126, (2019). https://doi.org/10.22033/ESGF/CMIP6.5743.

[48] N.C. Swart, J.N.S. Cole, V.V. Kharin, M. Lazare, J.F. Scinocca, N.P. Gillett, J. Anstey, V. Arora, J.R. Christian, Y. Jiao, W.G. Lee, F. Majaess, O.A. Saenko, C. Seiler, C. Seinen, A. Shao, L. Solheim, K. von Salzen, D. Yang, B. Winter, M. Sigmond, CCCma CanESM5 model output prepared for CMIP6 ScenarioMIP ssp126, (2019). https://doi.org/10.22033/ESGF/CMIP6.3683.

[49] S. Yukimoto, T. Koshiro, H. Kawai, N. Oshima, K. Yoshida, S. Urakawa, H. Tsujino, M. Deushi, T. Tanaka, M. Hosaka, H. Yoshimura, E. Shindo, R. Mizuta, M. Ishii, A. Obata, Y. Adachi, MRI MRI-ESM2.0 model output prepared for CMIP6 ScenarioMIP ssp126, (2019). https://doi.org/10.22033/ESGF/CMIP6.6909.

[50] O. Boucher, S. Denvil, G. Levavasseur, A. Cozic, A. Caubel, M.-A. Foujols, Y. Meurdesoif, P. Cadule, M. Devilliers, E. Dupont, T. Lurton, IPSL IPSL-CM6A-LR model output prepared for CMIP6 ScenarioMIP ssp126, (2019). https://doi.org/10.22033/ESGF/CMIP6.5262.

[51] H. Shiogama, M. Abe, H. Tatebe, MIROC MIROC6 model output prepared for CMIP6 ScenarioMIP ssp585, (2019). https://doi.org/10.22033/ESGF/CMIP6.5771.

[52] N.C. Swart, J.N.S. Cole, V.V. Kharin, M. Lazare, J.F. Scinocca, N.P. Gillett, J. Anstey, V. Arora, J.R. Christian, Y. Jiao, W.G. Lee, F. Majaess, O.A. Saenko, C. Seiler, C. Seinen, A. Shao, L. Solheim, K. von Salzen, D. Yang, B. Winter, M. Sigmond, CCCma CanESM5 model output prepared for CMIP6 ScenarioMIP ssp585, (2019). https://doi.org/10.22033/ESGF/CMIP6.3696.

[53] S. Yukimoto, T. Koshiro, H. Kawai, N. Oshima, K. Yoshida, S. Urakawa, H. Tsujino, M. Deushi, T. Tanaka, M. Hosaka, H. Yoshimura, E. Shindo, R. Mizuta, M. Ishii, A. Obata, Y. Adachi, MRI MRI-ESM2.0 model output prepared for CMIP6 ScenarioMIP ssp585, (2019). https://doi.org/10.22033/ESGF/CMIP6.6929.

[54] O. Boucher, S. Denvil, G. Levavasseur, A. Cozic, A. Caubel, M.-A. Foujols, Y. Meurdesoif, P. Cadule, M. Devilliers, E. Dupont, T. Lurton, IPSL IPSL-CM6A-LR model output prepared for CMIP6 ScenarioMIP ssp585, (2019). https://doi.org/10.22033/ESGF/CMIP6.5271.

[55] C. Alfsdotter, A. Petaros, Outdoor human decomposition in Sweden: a retrospective quantitative study of forensic-taphonomic changes and postmortem interval in terrestrial and aquatic settings, J. Forensic Sci. 66 (2021) 1348–1363, https://doi.org/10.1111/1556-4029.14719.

[56] R. Wu, J. Chen, Z. Wen, Precipitation-surface temperature relationship in the IPCC CMIP5 models, Adv. Atmos. Sci. 30 (2013) 766–778, https://doi.org/10.1007/s00376-012-2130-8.

[57] IPCC, Climate Change 2014 Part A: Global and Sectoral Aspects, 2014. papers2://publication/uuid/B8BF5043-C873–4AFD-97F9-A630782E590D.